RSC Advances

PAPER

View Article Online
View Journal | View Issue

Cite this: *RSC Adv.*, 2024, **14**, 6112

Recovery of potassium salt by acidification of crude glycerol derived from biodiesel production

Leily Nurul Komariah, * Susila Arita, Lia Cundari and Bazlina Dawami Afrah

Crude glycerol (CG) is a major byproduct of biodiesel production. Most of it cannot be utilized due to major impurities. The CG generally contains alkalis, which generate the residual salts in a series of its purification stages. This study aims to obtain the optimum process conditions and acid molar ratio to produce a higher potassium salt yield while improving the purity of glycerol by a simple acidification procedure. The CG was obtained from the transesterification of palm oil using a catalyst based on potassium carbonate. A phosphoric acid (85%) is utilized at various molar ratios and the process temperature is 60–80 °C. The strong acid was slowly added to the CG and heated for 30 minutes with a mixing speed of 250 rpm. The optimum acidification process occurred at a temperature of 70 °C with a molar crude glycerol ratio to phosphoric acid of 1 : 0.5. The glycerol purity was increased from 43.3% to 67.63% (w/w). It effectively obtains a potassium phosphate salt with a yield of 6.78%. The functional group infrared (IR) and X-ray fluorescence (XRF) spectra identified the salt residue as potassium dihydrogen phosphate (KH_2PO_4). This is composed predominantly of potassium oxide (K_2O) and phosphorus pentoxide (P_2O_5), 50% and 47.9%, respectively.

Received 4th December 2023
Accepted 2nd February 2024

DOI: 10.1039/d3ra08264d

rsc.li/rsc-advances

1 Introduction

The biodiesel industry has grown significantly due to the need for alternative fuels. Globally, both demand and production of biodiesel has been increasing steadily. The United States, Indonesia, and Brazil are the world's largest producers of biodiesel which is typically produced from rape seed, sunflower, coconut, soybean, oil palm, and jatropha. The most common technology for making biodiesel is transesterification with a homogenous alkaline catalyst.

Biodiesel production generates about 10% (w/w) glycerol as the main by-product. As its production continues to increase, the projected amount of crude glycerol will also increase. Currently, 10% of glycerol is generated from hydrolysis, 12% glycerol from saponification and 50–80% glycerol from the transesterification process or biodiesel production.[1] Biodiesel production is becoming the biggest driver of glycerol in the last few years. Allied Market Research reported that the significant growth in biodiesel production is driving the market growth of glycerol. Biodiesel dominated the glycerol market with a share of 59.5% in 2022.

Glycerol or glycerine is a versatile compound that can be converted into many derivative products. It has been identified as one of the 12 most important bio-based chemicals in the world.[2] Glycerol is generally used as a humectant in the food, beverage, and tobacco industries as well as being used as a solvent, a sweetener, and a thickening agent.[3] Glycerol is generally marketed at a purity level of >80%. In order to increase its purity, a series of CG processes are needed according to the original conditions or its contents.

The glycerol plays a vital role in industry. Glycerol can be marketed commercially in a crude and a refined form. Most of the glycerol that is supplied on the market is derived from oleochemicals (fatty acids, fatty alcohols, soap) and the biodiesel industries.

Many research institutions have given similar forecasts about having the potential for a strong glycerol market in the future. The global glycerol market is projected to continue growing. It is estimated to be valued at US$ 2.91 billion in 2022 and is expected to exhibit a compound annual growth rate (CAGR) of 7.4% over the forecast period (2023–2030). As a result, about 6.3 million tonnes of crude glycerol will be produced by 2025.[4] Several research institutes reported that the global glycerol market size was valued at USD 4.87 billion in 2022 and this is estimated to reach USD 3.18 billion in 2023, and the revenue forecast for 2030 will reach USD 5.67 billion.

The glycerol content in a crude glycerol is commonly in 30–60% (w/w).[5–7] This is far below that of purified glycerol.[8] Glycerol from biodiesel production is generally found to have impurities. Its composition mainly depends on the raw materials, the oil and methanol molar ratio, the type of catalyst used, and the detailed transesterification procedure.[4,9,10]

Typical impurities in crude glycerol are water/moisture, ash (*i.e.*, inorganic salts), and matter organic non-glycerol (MONG), which usually consists of free fatty acids (FFAs), fatty acid

Department of Chemical Engineering, Faculty of Engineering, Universitas Sriwijaya, 30662 Indralaya, Ogan Ilir, Indonesia. E-mail: leilynurul@unsri.ac.id

Table 1 Summary of glycerol purification technologies

Technology used	Glycerol purity (%) Initial	Final	Residual salt type, recovery (%)	Ref.
Acidification, neutralization, extraction	13%	96%	KH_2PO_4; 5.6% by wt K_2HPO_4	13
Liquid–liquid extraction (neutralization), distillation, adsorption	30%	62%	Not defined, <6%	14
Saponification, acidification, phase separation and extraction, membrane filtration, adsorption	40%	93.7%	Not defined, 5–7%	15
Neutralization ion exchange, membrane separation, desalination, distillation–dehydration	—	95%	Na_2SO_4, n.d.	16
Acidification, polar solvent extraction, activated carbon adsorption	—	95.74%	n.d.	17
Acidification, neutralization, vacuum distillation	30.3%	93.34%	n.d., 5.16%	18
Neutralization, centrifugation, evaporation, ion exchange, vacuum distillation	—	98%	n.d.	2
Acidification, neutralization, vacuum distillation, membrane separation, adsorption, ion exchange	40%	97.5%	5–7%	19
Acidification, neutralization, decolorization, solvent extraction, adsorption	23.3%	92.5%	2.1%	20
Decomposition of glycerol with HCl, splitting, adsorption	—	95%	0.95% natrium salts	21

methyl esters (FAME), glycerides, alcohols such as methanol or ethanol, and soaps and other organic compounds.[4,8,11,12] The impurities existing in the natural raw feedstocks tend to accumulate in the glycerol phase after the reaction. Consequently, the treatment scheme to purify crude glycerol is commonly based on chemical and physical operations or a combination of them.

Glycerol purification involves multiple unit operations. It is generally a physicochemical treatment comprising saponification, acidification, phase separation, and extraction to remove most impurities. The summary of glycerol purification technologies is presented in Table 1. Advanced technologies are employed to purify crude glycerol, including vacuum distillation,[22–24] ion exchange,[25,26] membrane separation,[15,27] adsorption,[28–30] electrodialysis,[4] and membrane distillation.[31] All of these techniques succeeded in increasing the purity of glycerol, although only some of the methods yielded more than 90% purity as expected. Recently, the multiple routes for glycerol purification are considered when designing biodiesel plants.[10]

As is known, purification processes of crude glycerol generally require significant energy input, are high in chemical consumption, and have high production costs.[32] Distillation of crude glycerol and the process combination are energy intensive processes due to the high specific heat capacity of glycerol that leads to a high-energy input requirement for vaporization and to create thermal decomposition.[24] Therefore, the glycerol residue from the biodiesel process is often disposed of[14,20] or accumulates in landfill.[33] Sometimes it is considered waste due to its low purity for industrial applications.

Some challenges in crude glycerol utilization are resolved without a complex and high-cost process. Several researchers have reported that crude glycerol with a low purity can be used directly as a fuel[8] or with another energy source, such as syngas, bio-char, bio-oil, biogas, hydrogen, and alcohol.[8,34] Crude glycerol is also effective as an animal feedstuff.[2] However, those uses have not been widely implemented and have yet to be integrated into biodiesel production units.

There have been several attempts to convert the impurities present in CG to valuable products. One is converting residual catalysts into organic salts by selecting the proper acid in the acidification and neutralization process, as reported by several authors.[14,20,21,35]

Another technology used for the purification of glycerol with a high salt content is to use ion-exchange.[9] Salts are by-products and, can be used as potash-phosphate fertilizer. Work done by Enilson *et al.*[33] evaluated the use of the glycerin effluent, a waste from the transesterification of triacylglycerides catalyzed with KOH, as a potassium source to increase the yield of crops. It was assayed as fertilizer for soils supporting the growth of soybean plants.

The basic step during CG treatment is its decomposition by a strong mineral acid.[21] From this stage the salt content in crude glycerol commonly ranged from 5% to 8% wt.[21,26,36] This portion is equivalent to the catalyst consumption required in biodiesel production. The formation of higher levels of salts eventually deposit into a crude glycerol layer.[10]

Phosphoric acid (H_3PO_4) was chosen for the acidification process because it has a better separation performance than other acids.[13,37–39] Acidification using phosphoric acid completely removed the soap and the catalyst from the crude glycerol.[5]

The challenge for glycerol purification technology is to use simple and concise processing techniques while simultaneously effectively increasing glycerol purity levels and producing valuable residual salts. The next challenge is to find a technology to utilize glycerol with a medium purity (60–90%) as a raw material for other economically valuable products. Therefore, in this study, CG was processed by only applying acidification using phosphoric acid at various processing temperatures and molar ratios of CG to the acid. Furthermore, the salt formed is identified to meet the criteria for use as economically valuable products. The purity of glycerol is also measured, and its utilization potential is assessed without further costly purification stages. An effective and efficient transformation of crude

glycerol into valuable products may contribute positively to the biodiesel economy.

2 Materials and method

The crude glycerol used in this study was produced from the transesterification of refined bleached deodorized palm oil (RBDPO) with excess methanol using a potassium carbonate-based catalyst. A scheme of the crude glycerol treatment process is shown in Fig. 1.

The acidification stage is carried out in a glass reactor placed on the hot plate stirrer. The stirring speed is set at 250 rpm. The acid used was H_3PO_4 85% in H_2O, 99.99% trace metals base (Sigma-Aldrich). At the initial stage, the molar ratio of crude glycerol : H_3PO_4 = 1 : 0.5, and the contact time is 30 minutes.

Various processing temperatures were used: room temperature, 60 °C, 70 °C, and 80 °C. Furthermore, the samples produced at the best conditions were retested using variations of the molar ratio of crude glycerol : H_3PO_4, 1 : 0.25, 1 : 0.5, 1 : 0.75, and 1 : 1.0.

After the acidification and decantation stages, the formation of the layers was examined. The fatty acid phase is found in the top layer, followed by glycerol-rich and inorganic salt phases in the middle and bottom, respectively. The top phase was separated from the glycerol-rich phase by using a separator funnel. The bottom phase then was separated by simple decantation, and this process lasted 18–24 hours. The liquid content in this solid residue was then evaporated at a temperature of 90 °C for 2 hours, and this was followed by drying in the oven at a temperature of 65 °C for 60 minutes. The composition and physical properties of the middle layer or glycerol-rich mixture were then identified based on density, moisture content, pH, ash content, and glycerol content.

Table 2 shows the analysis method used. Meanwhile, a series of analyses were carried out on the resulting solid residues as presented in Table 3.

Table 2 Analysis methods of the physical properties of crude glycerol and treated glycerol

Parameter	Unit	Method/standard
Physical appearance	—	Color/observation
Density	kg m^{-3}	ASTM D4062
Water content	ppm	Karl Fischer titration
Free fatty acids (FFA)	%	Calculated from acid value – ASTM D664
pH	—	pH meter (Metrohm)
Ash content	%	ISO 2098-1972
Glycerol content	%	Gas chromatography

Table 3 Methods of the analysis of residual salt

Parameter	Method/standard
Physical appearance	Color/observation
Density	ASTM D4062
Water content	Karl Fischer titration
Functional group	Fourier transform infrared spectroscopy (FTIR)
Morphology	SEM
Elemental identification	X-ray fluorescence analysis (XRF)
Purity	Titration, GC/MS based

3 Results and discussion

3.1 Effects of temperature and layer formation

Temperature is one factor which determines the success of the acidification process. Fig. 3 shows a schematic of some of the compounds formed after CG acidification. In this step, phosphoric acid (H_3PO_4) was added slowly to improve the acidity of the crude glycerol with various temperatures. Previously, the CG was preheated at a specified process temperature. In general, the addition of phosphoric acid at various temperatures causes

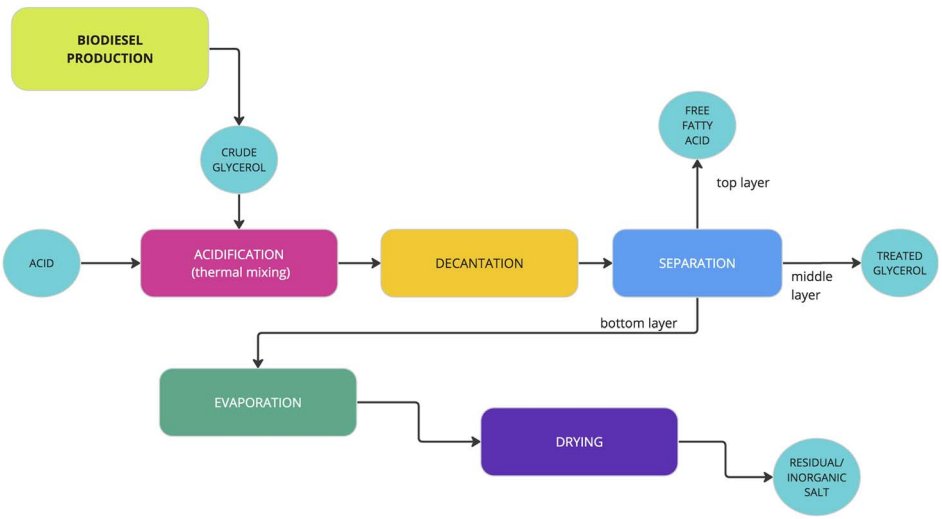

Fig. 1 Scheme of crude glycerol purification.

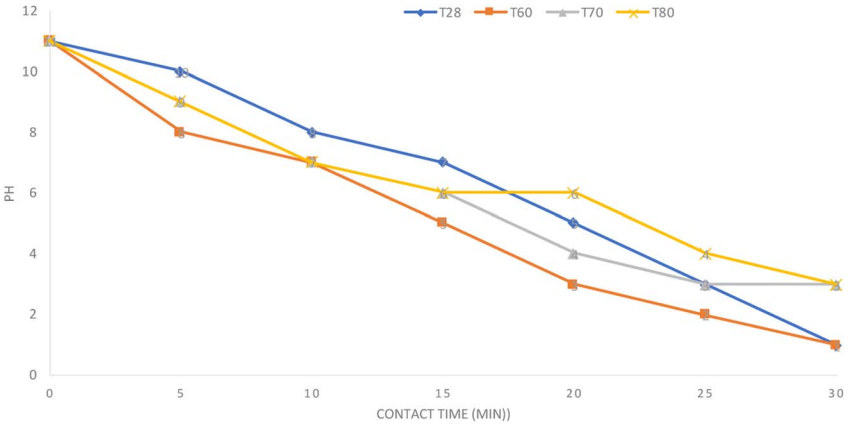

Fig. 2 The pH reduction profile during the crude glycerol acidification process.

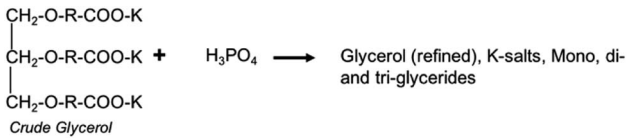

Fig. 3 The acidification of crude glycerol.

differences in the numbers of layer detected after process, as seen in Table 4.

When an acid is dissolved in a solution, it furnishes hydrogen ions, and consequently, the concentration of hydrogen ions increases. The reaction is highly exothermic in nature due to the production of heat. Increasing the temperature increases the average speed of the reactant molecules. The reaction rate of the reactant molecules increases as the temperature rises. The number of molecules that are able to react quickly rises as more molecules move more quickly, hastening the creation of the products.

The reaction of glycerol with phosphoric acid generates heat, but at 80 °C, the salt formed was dissolved and mixed back into the glycerol-rich phase. It is known that the moisture content in the glycerol phase is sufficient to re-dissolve the salt. On the other hand, during the adification process, there was a change in the temperature of the CG mixture, but this pattern was relatively not identical to the decrease in pH, as seen in Fig. 2.

Mixtures that reach a pH between 2 and 3 faster are those processed at 60 °C. But at the end of the neutralization and separation process, the mixture only shows the formation of 2 layers, namely fatty acid and glycerol phases. This condition indicates that the solid residue that should have separated has dissolved back into the glycerol phase due to mixing. This is a similar pattern to that which occurs in mixtures processed at 80 °C. The decreasing trend of ash and matter organic non-glycerol (MONG) contents occurred with the decrease of the pH.[13] A very low acidity will cause residual solids containing short-chain and medium-chain fatty acids to easily dissolve in the glycerol phase, especially when the stirring continues. The mixture formed from the process at 70 °C showed the formation of three distinct layers (Table 4). The bottom layers contain solids, phosphate salts, and MONG.

The crude glycerol appearance after acidification is presented in Fig. 4. The number of layers and boundaries of each layer are observed to estimate the effectiveness of the pretreatment process that had been carried out. The process that took place at a temperature of 70 °C showed the formation of three layers consisting of FFA at the top, a turbid glycerol-rich liquid in the middle, and solid residues in the lower layer.

The addition of phosphoric acid at 70 °C was able to neutralize alkaline catalyst residues and break down soap into free fatty acids and salt. When the temperature is increased, it increases the kinetic energy of the molecules. This tends to increase the ionization and more water is converted to H^+ and OH^- ions. Hence, the pH and pOH decrease with increasing temperature. Water dissociates into ions more at higher temperatures, leading to a higher concentration of hydrogen

Table 4 Comparison of mixed conditions after acidification

Process temperature	T_0 = room temperature	T_1 = 60 °C	T_2 = 70 °C	T_3 = 80 °C
Number of layers detected	2	2	3	2
Glycerol phase pH	2	2	3	3
Top layer (free fatty acid)	Aqueous foam (high)	Aqueous foam (high)	Aqueous foam (high)	Aqueous foam (medium)
Middle layer (glycerol phase)	Faint layer borders, turbid yellow	Dark yellow, the layer border is quite clear	Dark yellow, clearer, clear layer borders	Bright yellow, cloudy, faint layer border
Bottom layer (residues/ solids)	n.a.	n.a.	Detected	n.a.

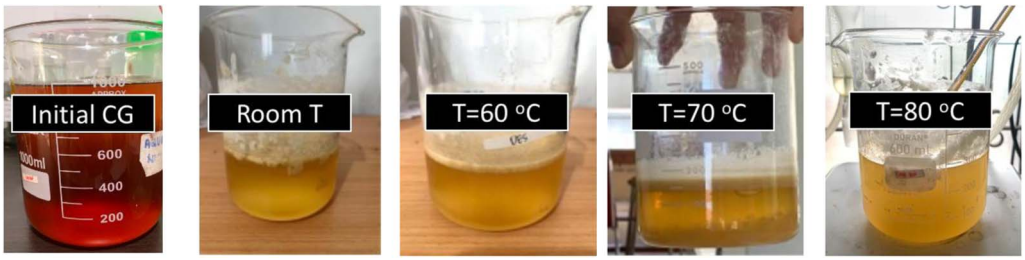

Fig. 4 Crude glycerol after the acidification process with H_3PO_4.

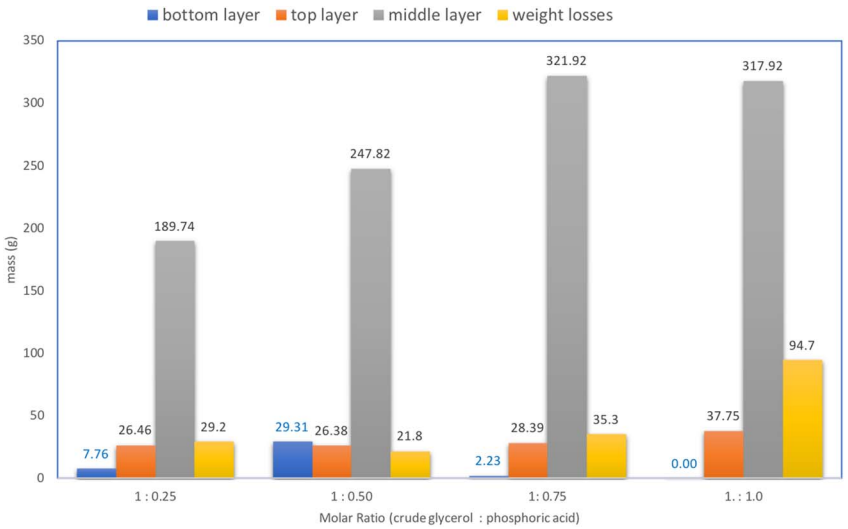

Fig. 5 Mass comparison of each layer at CG after the acidification.

ions (or H_3O^+). A higher concentration of H_3O^+ ($[H_3O^+]$) results in a lower pH, but it does not mean that the acidity of the sample has changed.

The addition of H_3PO_4 leads to the low pH of the mixture. It is considered to be in an acidic atmosphere. As is known, chemical treatment at a low pH is better. It increased the glycerol and reduced the ash content in the recovered crude glycerol. On the other hand, the right dosage and process temperature cause phosphoric acid to bind successfully to the remaining potassium-based catalysts (K_2CO_3) and potassium soap that are formed.

Potassium ions from bases and soaps bind to phosphate ions to form salts. At the same time, the matter organic non-glycerol (MONG) content was slightly increased.

3.2 Effects on solid residue formation

The acidification process with a temperature of 70 °C was then used for various molar ratios of CG to H_3PO_4. As shown in Fig. 5, the mass balance and form of the layers are apparent after the treatment.

The acidification with molar ratios of 1 : 0.25 and 1 : 0.50 produce three noticeable layers. The most residue of the solids in the bottom layer was found with the molar ratio of 1 : 0.5. This suggests that the exact dosage of the acid is an important and decisive factor.

An excessive amount of acid will increase the solubility of the salts in glycerol, so the precipitate does not separate and the glycerol content in the middle layer will decrease. The soap content in the crude glycerol forms free fatty acids which are detected in the upper layers. Not all the soaps are converted to FFA, so the rest of the soap will muddy the glycerol phase and will remain in the residue, and then become impurities in the potassium salts.

As shown in Fig. 5, the acquisition of salt residues at the end of the acidification stage is mostly detected at the molar ratio of $CG : H_3PO_4 = 1 : 0.5$. After filtration and drying, there was 13.562 g of residual salt obtained in every 200 g of CG treated. The yield of potassium salt is considered to be 6.78% (w/w). Whereas, the middle layer of glycerol neutralized with NaOH then showed an increase in the original purity of 49.80% to 67.63% (w/w).

The addition of H_3PO_4 to CG has an interaction with the ash content and water content. In this work, the CG previously contained a moisture content of 30.9% (w/w). This condition is contributed by the hygroscopic nature of glycerol, which absorbs moisture from the surrounding environment during the transesterification process. After acidification, the moisture content increases to 34.4%. In the acidification process, the phosphoric acid reacts with K_2CO_3 as the spent catalyst, producing KH_2PO_4, CO_2, and water. Then the water will be in

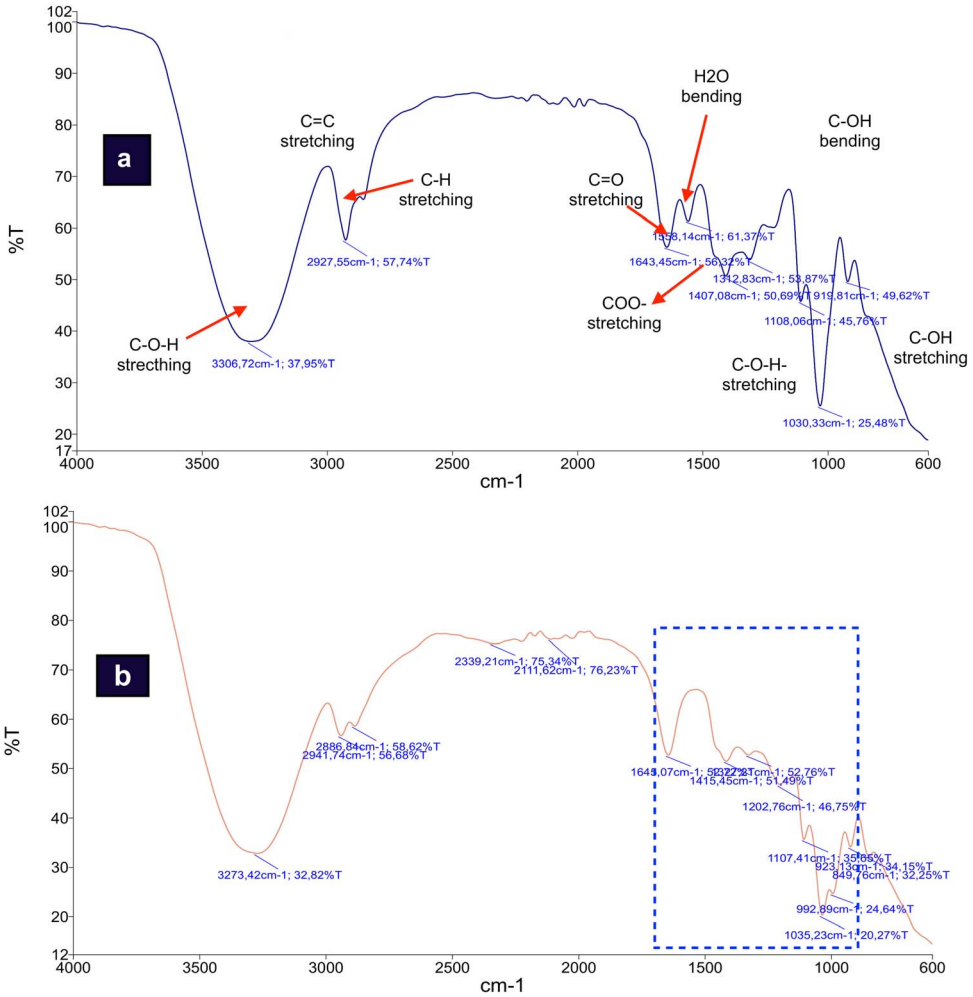

Fig. 6 Functional group changes between (a) crude glycerol and (b) glycerol-rich phase.

the glycerol phase. Consequently, the water contents tend to continue to increase, thereby reducing the purity of glycerol.

According to Manosak *et al.*[17] the ash content in the glycerol-rich layer was higher than the original levels in crude glycerol due to the process being under strongly acidic conditions. The ash content of the CG began at a level of 4.63%. After acidification, the ash content was 10.31% by wt. KH_2PO_4 in the pH range of 2–4 generated from the complexing of potassium ions from the contaminated salts in the crude glycerol. It is also generated from the excess PO_4^{2-} ionized from $H_2PO_4^-$. KH_2PO_4 is soluble in water and tend to be in crude glycerol–water acid phase. These findings provide further research opportunities to increase the yield of potassium salts by controlling the pH at optimum intervals.

3.3 Functional group changes in crude glycerol

The comparison or transitions in functional groups between the initial crude glycerol and crude glycerol after the acidification stage is shown in Fig. 6. This change indicates the effectiveness of the use of phosphoric acid at 70 °C processing conditions against the reduction of impurities present in CG.

The most significant difference between the initial crude glycerol spectrum (CG_0) and CG after acidification (CG*) is the number of peaks detected. Where the CG* shows 14 peaks, the CG_0 shows 9 peaks. The addition of phosphoric acid at a temperature of 70 °C causes some significant changes in the functional groups, as can be seen from the shapes of the absorption bands and their intensity in each functional group.

As is known, glycerol is an alcoholic compound that has three hydroxyl groups (–OH). The strong absorption at 3273 cm^{-1} that corresponds to the group of alcohol with

Table 5 The identification and properties of residual salts

Parameter	Unit	Description
Phase, form	—	Solid, crystal
Color	—	White
Moisture content	%	0.31 ± 0.02
Density	g cm^{-3}	2.29 ± 0.09
Soluble in water		Yes
Soluble in methanol		No
pH in 1% solution		4.6 ± 0.21

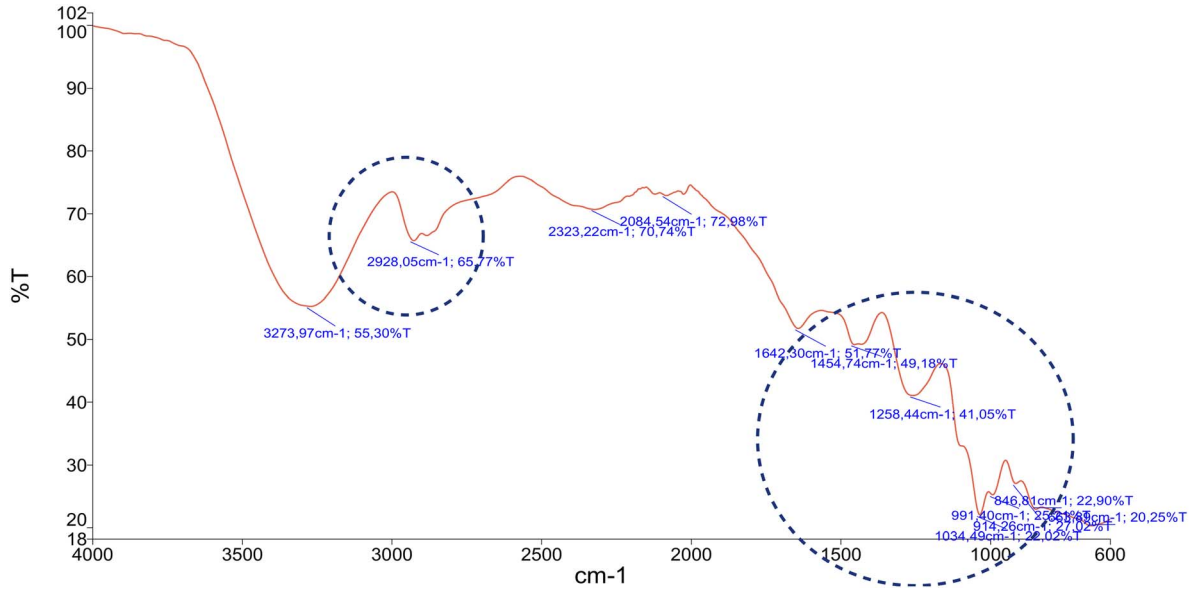

Fig. 7 FTIR spectrum of the potassium phosphate salt.

Table 6 The XRF analysis of the inorganic salt samples

Element			Natural state of sample (geology)			Oxides		
Compound	Conc.	Unit	Compound	Conc.	Unit	Compound	Conc.	Unit
P	28.534	%	P_2O_5	48.034	%	P_2O_5	47.984	%
K	68.558	%	K_2O	50.155	%	K_2O	50.073	%
Fe	0.042	%	Fe_2O_3	0.031	%	Fe_2O_3	0.031	%
Ag	2.833	%	Ag	1.762	%	Ag_2O	1.89	%
Ce	0.033	%	Ce	0.018	%	CeO_2	0.022	%

intermolecular bonded O–H stretching shows the predominance of the glycerol composition in the mixture. The presence of soap was detected by the signal at 1558 cm^{-1} corresponding to the carbonyl stretching of the carboxylate.

Functional groups and other groups of compounds appear as primary and secondary alcohol groups with C–O stretching frequencies at a region of 1030–1108 cm^{-1}, whereas groups represent the presence of the ester molecular groups as seen at the wavenumbers of 1202 cm^{-1} with strong C–O stretching. The H_2O bending at an area of 1645 cm^{-1} indicates the formation of a group of water molecules with a strong intensity.

The acidification of crude glycerol is very likely to produce CO_2, this is shown by detectable C═O═C bonds absorbed in the region of the infrared spectrum of 2339 cm^{-1}. From the broad visual patterns of the infrared spectra, in CG* several groups of compounds were detected, including the presence of a carbonyl functional group characterized by the presence (–COH) of stretching in the region of 2887 cm^{-1}. There are possibilities of the emergence of the alkyne group/ketene in the carbon–carbon triple bond stretch C≡C (duplicate 3) at 2111 cm^{-1} with a transmission of 76.2%. Various speculations about the CG reactions with H_3PO_4 exist. It may be related to the formation of alkyne compounds due to the hydration reaction of alkenes, where alkenes are formed due to the release of hydrogen from the alcohol group in CG. But another speculation was that the emergence of alkynes as unsaturated hydrocarbon compounds was due to the reaction of haloalkanes with the potassium compounds present in the CG.

3.4 Identification and characteristics of potassium salt

In this study, the RBDPO transesterification using a K_2CO_3-based catalyst, then acidification with H_3PO_4 produced a granular white solid that was considered to be potassium dihydrogen phosphate (KH_2PO_4). The possible reaction equation hypothesized is shown in eqn (1). In the acidification process, H^+ ions from phosphoric acid converted the soap to insoluble free fatty acids and an inorganic salt layer.[40]

$$K_2CO_3 + 2H_3PO_4 \rightarrow 2KH_2PO_4 + CO_2 + H_2O \quad (1)$$

Potassium-based salts obtained after the acidification stage are processed by the stages of filtration, evaporation, and drying.

Next, the a sample of the solids is analysed to determine the number of properties as presented in Table 5. The FTIR spectra

were also used to identify samples of the potassium salts produced, as shown in Fig. 7.

It is confirmed that there is potassium dihydrogen phosphate in the salt residue because the formation of peaks in the region's position corresponds to the IR spectra for the potassium phosphate salt. The form and peak position of the absorption and intensity of the absorption reinforce the argument about the constituent compounds of these residual salts.

The band at 2928 cm^{-1} corresponds to the O–H stretching vibration which emphasizes the presence of a hydroxyl functional group. It shows the spectral profile of KH_2PO_4 as reported by several authors.[41,42]

Specific to the product in this study, group vibration (PO_4) with a significant absorption intensity was found in the regions of 846 cm^{-1}, 914 cm^{-1}, 1258 cm^{-1}, and 1454 cm^{-1}. Region 846 cm^{-1} is an indication of the presence of a group $PO_2(H_2)$ vibration. The transmittance values among the wavenumber regions between 840–1500 cm^{-1} show the variety of vibrations with a medium absorption intensity.

3.5 Elemental analysis

The XRF spectrometry was used here to configure the elements in the salt product, and the results can be seen in Table 6. The salt element is dominated by potassium and phosphorus of 68.5% and 28.5% (w/w), respectively. While in the form of oxide, this salt contains 50% K_2O and 47.9% P_2O_5.

The composition of trace elements and oxides in the salt products is already ideal to qualify as a commercial fertilizer. The commercial ZK fertilizer requires a minimum K_2O content of 50%. According to the official standard of commercial fertilizers, the fertilizer must have more than 20% K_2O.[40] These phosphoric fertilizers with water-dissolved phosphorus acids include superphosphate (16–20% P_2O_5), and double or triple superphosphate (32–48% P_2O_5).

4 Conclusions

Crude glycerol from biodiesel production was treated in this study using simple acidification without further complex processes. Acidification is performed as an initial and decisive method to minimize the residual impurity present in crude glycerol. The acid used was phosphoric acid (85%). The best operating conditions are a temperature of 70 °C, stirring at 250 rpm for 30 minutes, with a molar ratio of $CG : H_3PO_4 = 1 : 0.50$. To obtain three distinct layers after the process, the acidity of the mixture was kept at a pH of 3–4. This procedure is considered effective for CG treatment by increasing by 35.8% the purity of glycerol compared to the initial condition. It also simultaneously generated a potassium salt with a yield of 6.78% (w/w). The salt formed is a white crystal that was successfully identified as potassium dihydrogen phosphate (KH_2PO_4) and contains 50% K_2O and 47.9% P_2O_5. This composition qualifies for commercialization as a fertilizer, thereby increasing the added value and bargaining position for the crude glycerol. This study showed that the purification of CG possibly does not always have to go through long stages of processing, which are complex, energy-intensive, and have heavy chemical consumption. Although it has not yet reached the maximum level of purity, this short and simple method has the potential to be applied on an industrial scale. Glycerol, with a purity of 67.63% (w/w), is acceptable for use as a raw material for energy production. It is encouraged by the existence of a glycerol market at low purity levels (<80%).

Author contributions

Leily Nurul Komariah: conceptualization, data curation, formal analysis, methodology, validation, visualization, writing – original draft. Susila Arita: methodology, data curation, writing review. Lia Cundari: project administration, resources, software, writing review & editing. Bazlina Dawami Afrah: project administration, resources, writing review & editing.

Conflicts of interest

There are no conflicts to declare.

Acknowledgements

The author appreciates the support of research facilities from the Indonesian Palm Oil Plantation Fund Management Agency (BPDPKS) and the Indonesian Biofuel Producers Association (APROBI) as well as all parties at the Laboratory of Energy Engineering Universitas Sriwijaya – Indonesia.

References

1 J. Kaur, A. K. Sarma, M. K. Jha and P. Gera, *Biotechnol. Rep.*, 2020, **27**, e00487.
2 S. S. Konstantinović, B. R. Danilović, J. T. Ćirić, S. B. Ilić, D. S. Savić and V. B. Veljković, *Chem. Ind. Chem. Eng. Q.*, 2016, **22**, 461–489.
3 S. C. Moldoveanu, *Pyrolysis of Alcohols and Phenols*, 2019.
4 T. Attarbachi, M. Kingsley and V. Spallina, *Fuel*, 2023, **340**, 127485.
5 L. R. Kumar, S. K. Yellapu, R. D. Tyagi and X. Zhang, *Bioresour. Technol.*, 2019, **293**, 1–30.
6 S. Naimah and E. Ratnawati, *Jurnal Kimia dan Kemasan*, 2010, **32**, 62.
7 A. Kovács, *Pet. Coal*, 2011, **53**, 91–97.
8 Y. Liu, B. Zhong and A. Lawal, *RSC Adv.*, 2022, **12**, 27997–28008.
9 M. Hájek and F. Skopal, *Bioresour. Technol.*, 2010, **101**, 3242–3245.
10 M. Kosamia, M. Samavi, B. K. Uprety and S. K. Rakshit, *Catalysts*, 2020, **10**, 1–20.
11 H. Dewajani, A. R. Hakim, M. A. I. Iswara, T. Susanti and D. Pratiwi, *IOP Conf. Ser.: Mater. Sci. Eng.*, 2020, **732**, 1–9.
12 V. Y. Mena-Cervantes, R. Hernández-Altamirano and A. Tiscareño-Ferrer, *Environ. Sci. Pollut. Res.*, 2020, **27**, 28500–28509.
13 Z. Nanda, M. Yuan, W. Qin and C. M. A. Poirier Xu, *Austin Chem. Eng.*, 2015, **1**, 1–7.

14 F. D. Pitt, A. M. Domingos and A. A. C. Barros, *S. Afr. J. Chem. Eng.*, 2019, **29**, 42–51.
15 C. G. Chol, R. Dhabhai, A. K. Dalai and M. Reaney, *Fuel Process. Technol.*, 2018, **178**, 78–87.
16 P. Vadthya, A. Kumari, C. Sumana and S. Sridhar, *Desalination*, 2015, **362**, 133–140.
17 R. Manosak, S. Limpattayanate and M. Hunsom, *Fuel Process. Technol.*, 2011, **92**, 92–99.
18 S. Kongjao, S. Damronglerd and M. Hunsom, *Korean J. Chem. Eng.*, 2010, **27**, 944–949.
19 R. Dhabhai, P. Koranian, Q. Huang, D. S. B. Scheibelhoffer and A. K. Dalai, *Sep. Sci. Technol.*, 2023, **58**, 1383–1402.
20 K. A. V. Miyuranga, U. S. P. R. Arachchige, R. A. Jayasinghe and G. Samarakoon, *Energies*, 2022, **15**, 2–22.
21 T. Kocsisová and J. Cvengroš, *Pet. Coal*, 2006, **48**, 1–5.
22 M. Oliveira, A. Ramos, E. Monteiro and A. Rouboa, *Sustainability*, 2022, **14**, 3–12.
23 O. S. Muniru, C. S. Ezeanyanaso, E. U. Akubueze, C. C. Igwe and G. N. Elemo, *J. Energy Res. Rev.*, 2018, 1–6.
24 H. W. Tan, A. R. Abdul Aziz and M. K. Aroua, *Renew. Sust. Energ. Rev.*, 2013, **27**, 118–127.
25 A. A. Abdul Raman, H. W. Tan and A. Buthiyappan, *Front. Chem.*, 2019, **7**, 1–9.
26 P. Pal and S. P. Chaurasia, *Vth International Symposium on "Fusion of Science & Technology*, 2016, pp. 393–397.
27 I. M. Atadashi, *Alex. Eng. J.*, 2015, **54**, 1265–1272.
28 E. Anzar, S. Yusi and Y. Bow, *Indones. J. Fundamental Appl. Chem.*, 2018, **3**, 83–88.
29 S. Chozhavendhan, K. P. Kumar, P. Sable, R. Subbaiya, G. K. Devi and S. Vinoth, *Res. J. Pharm. Technol.*, 2019, **12**, 649–654.
30 M. Hunsom, P. Saila, P. Chaiyakam and W. Kositnan, *Int. J. Renew. Energy Res.*, 2013, **3**, 364–371.
31 M. M. A. Shirazi, A. Kargari, M. Tabatabaei, A. F. Ismail and T. Matsuura, *Chem. Eng. Process.: Process Intensif.*, 2014, **78**, 58–66.
32 S. S. Win and T. A. Trabold, *Sustainable Waste-To-Energy Technologies: Transesterification*, Elsevier Inc., 2018.
33 B. S. de Enilson, N. H. Elton, H. G. Paulo, D. F. Jose and T. C. Alessandro, *Afr. J. Agric. Res.*, 2015, **10**, 1572–1580.
34 Q. (Sophia) He, J. McNutt and J. Yang, *Renew. Sust. Energ. Rev.*, 2017, **71**, 63–76.
35 A. Choirun Az Zahra, I. Arina Rusyda, A. Hizbiyati, F. Giovani, N. Zahara, B. Jiwandaru, D. Gunawan, G. Andre Halim, M. Pratiwi, A. Nur Istyami, A. Verani Rouly Sihombing, A. Harimawan, D. Sasongko and J. Rizkiana, *IOP Conf. Ser.: Mater. Sci. Eng.*, 2021, **1143**, 012030.
36 F. Yang, M. A. Hanna and R. Sun, *Biotechnol. Biofuels*, 2012, **5**, 1–10.
37 R. Mythili, P. Venkatachalam, P. Subramanian and D. Uma, *Fuel*, 2014, **117**, 103–108.
38 Z. Nanda, M. Yuan, W. Qin and C. M. A. Poirier Xu, *Austin Chem. Eng.*, 2015, **1**, 1–7.
39 N. Saifuddin, H. Refal and P. Kumaran, *Res. J. Appl. Sci. Eng. Technol.*, 2014, **7**, 593–602.
40 S. Sadhukhan and U. Sarkar, *Energy Convers. Manag.*, 2016, **118**, 450–458.
41 E. Alshamaileh, M. R. Al-Rbaihat, B. Al-Saqarat, B. Udvardi and A. E. Al-Rawajfeh, *J. Eng.*, 2019, 81–93.
42 C. Sun, D. Xu and D. Xue, *Mater. Res. Innov.*, 2014, **18**, 370–375.